

Density-functional investigation of $\text{Na}_{16}\text{A}_8\text{Ge}_{136}$ (A = Rb, Cs) clathrates

Koushik Biswas¹ and Charles W Myles

Department of Physics, Texas Tech University, Lubbock, TX 79409-1051, USA

E-mail: koushik.biswas@nrel.gov

Received 1 August 2007, in final form 16 September 2007

Published 23 October 2007

Online at stacks.iop.org/JPhysCM/19/466206

Abstract

We have studied the electronic and vibrational properties of the filled Ge-based clathrates, $\text{Na}_{16}\text{Rb}_8\text{Ge}_{136}$ and $\text{Na}_{16}\text{Cs}_8\text{Ge}_{136}$. We have performed calculations using the generalized gradient approximation (GGA) to density-functional theory. Both materials are found to have metallic character, in agreement with experimental data. The predicted phonon dispersion curves show the low frequency, localized ‘rattling’ modes of the guest atoms. The calculated frequencies of these guests are in good agreement with experimentally estimated values. We have used the GGA calculated frequencies to estimate the temperature dependent isotropic atomic displacement parameter (U_{iso}) of the different guest atoms. The temperature dependences of the estimated U_{iso} are also consistent with experiment. We predict that the Rb guests in $\text{Na}_{16}\text{Rb}_8\text{Ge}_{136}$ have larger U_{iso} than Cs in $\text{Na}_{16}\text{Cs}_8\text{Ge}_{136}$, in agreement with experiment. This work shows that harmonic approximation based density-functional calculations may be used both to predict relatively accurate vibrational frequencies of the various guest atoms and to estimate the localized dynamic disorder created by such atoms at finite temperatures.

1. Introduction

Thermoelectric effects can have practical applications in the fields of alternative power generation (Seebeck effect) or as environmentally friendly refrigeration and cooling devices in modern electronics (Peltier effect). However, their performance depends on the specific properties of the materials that are used to build these devices.

Much of the current research on thermoelectric materials has revolved around the concept of the ‘phonon glass-electron crystal’ (PGEC) model proposed by Slack [1]. This concept suggests that good thermoelectric materials should have the electronic properties of a crystalline material and the thermal properties of a glass. Group-IV clathrates have emerged as a promising

¹ Present address: National Renewable Energy Laboratory, Golden, CO 80401, USA.

class of materials that fits into phases the PGEC concept [2]. These are expanded volume, cage-like phases of Si or Ge with Group-I or Group-II guest atoms encapsulated inside the cages. Group-IV clathrates are classified into two categories: type-I and type-II. The type-I structure is simple cubic and is made up of 20-atom cages and 24-atom cages that are arranged periodically in a 1 to 3 ratio [3]. Type-II clathrates, on the other hand, have a face-centred cubic (fcc) structure with 20- and 28-atom cages combined in a 2 to 1 ratio [3].

Type-II clathrates have not been as widely investigated as the type-I variety. However, several experimental and theoretical studies have recently been reported on the type-II Si and Ge clathrates [2, 4–9]. One unique characteristic of the type-II clathrate structure is the two different sized cages, which may be partially or completely filled by a single type of guest atom or by two different atom types [3, 8–11]. Depending on the nature and concentration of the guest atoms, the electronic and vibrational properties of these materials may be altered such that they can be potentially useful in thermoelectric devices [1, 2].

In this paper, we report a theoretical study of the electronic and vibrational properties of the completely filled $\text{Na}_{16}\text{Rb}_8\text{Ge}_{136}$ and $\text{Na}_{16}\text{Cs}_8\text{Ge}_{136}$ clathrates. Our electronic band structure calculations show that both $\text{Na}_{16}\text{Rb}_8\text{Ge}_{136}$ and $\text{Na}_{16}\text{Cs}_8\text{Ge}_{136}$ are metallic, in agreement with experimental results [8, 9]. The phonon dispersion curves show low frequency, guest atom ‘rattling’ modes for each material. An accurate calculation of these rattler modes is important because these low frequency modes may scatter the host acoustic phonons, potentially reducing the lattice thermal conductivity. We note that the generalized gradient approximation (GGA)-predicted guest vibrational frequencies for $\text{Na}_{16}\text{Cs}_8\text{Ge}_{136}$ obtained in this study differ from those obtained earlier within the local density approximation [12]. Our generalized GGA-predicted guest vibrational frequencies are in good agreement with experimentally estimated values [9]. Using our calculated frequencies, we have also estimated the temperature dependent isotropic atomic displacement parameters (U_{iso}) of the guest atoms and have compared them with experimental data [9]. The temperature dependences of the predicted values are consistent with experiment and show that the Rb guests, even though they are smaller and lighter, have larger U_{iso} than the heavier Cs guests.

2. Computational details

Our calculations are based on the GGA to density-functional theory. We use a plane-wave basis and ultrasoft pseudopotentials [13]. The Vienna *ab initio* simulation package (VASP) [14] has been used to carry out the calculations. The exchange–correlation potential was that of Perdew and Wang [15]. First, we optimize the geometry of each material by choosing a fixed volume of the face-centred cubic unit cell and relaxing the internal coordinates of the atoms through a conjugate gradient algorithm using atomic forces. This process is repeated for several different unit cell volumes until the global minimum energy is found. Brillouin zone integrations are performed using a $4 \times 4 \times 4$ Monkhorst–Pack k -point grid [16], with a plane-wave cutoff energy of 300 eV. During the geometry optimization, the different force components are converged to within $0.0003 \text{ eV } \text{\AA}^{-1}$ or less. The resulting energy versus volume curves are then fitted to the Birch–Murnaghan equation of state (EOS) [17]. This fitting determines the minimum energy of the optimized structure (E_0), the corresponding volume (V_0) and the equilibrium bulk modulus (B). The electronic band structures and densities of states are calculated at the optimized geometry of each material by generating a separate set of k -points along certain high symmetry directions in the Brillouin zone.

The vibrational calculations are done using the harmonic approximation. The first step is to obtain the force constant matrix by moving each atom in the optimized structure by a small finite displacement, $\pm U_0(0.02 \text{ \AA})$. VASP allows the determination of the force constant matrix

Table 1. Calculated bulk moduli and lattice constants for $\text{Na}_{16}\text{Rb}_8\text{Ge}_{136}$ and $\text{Na}_{16}\text{Cs}_8\text{Ge}_{136}$. Experimental lattice constants are also shown [8, 18].

Clathrate	Bulk modulus (GPa), theory	Lattice constant (Å)	
		Theory	Expt
$\text{Na}_{16}\text{Rb}_8\text{Ge}_{136}$	49.4	15.35	15.48
$\text{Na}_{16}\text{Cs}_8\text{Ge}_{136}$	48.0	15.44	15.48

Table 2. Calculated and experimental [8, 18] nearest neighbour distances in $\text{Na}_{16}\text{Rb}_8\text{Ge}_{136}$ and $\text{Na}_{16}\text{Cs}_8\text{Ge}_{136}$.

Clathrate	Ge–Ge (Å)		Na–Ge (Å)		Cs–Ge (Å)		Rb–Ge (Å)	
	Theory	Expt	Theory	Expt	Theory	Expt	Theory	Expt
$\text{Na}_{16}\text{Rb}_8\text{Ge}_{136}$	2.47–2.49	2.4911– 2.510	3.32–3.51	3.3528– 3.5444			4.10–4.18	4.1331– 4.2192
$\text{Na}_{16}\text{Cs}_8\text{Ge}_{136}$	2.48–2.50	2.4859– 2.5033	3.34–3.53	3.3516– 3.5395	4.12–4.20	4.1356– 4.2173		

by calculating the Hessian matrix (the matrix obtained from the second derivatives of energy with respect to the atomic positions). We have used a $2 \times 2 \times 2$ k -point grid to calculate the Γ -point phonon modes. We have repeated the $\text{Na}_{16}\text{Rb}_8\text{Ge}_{136}$ calculations with a $4 \times 4 \times 4$ grid and the same cutoff energy. This did not produce any appreciable difference in the frequencies. The dynamical matrix is obtained from the Fourier transform of the force constant matrix. In order to obtain the dynamical matrix at non-zero wavevector, following previous work [6, 7], we have introduced an approximation which assumes that the force constant matrix elements vanish for atoms that are separated by a distance that is greater than the third nearest neighbour. Details of this method may be found in [6, 7]. Diagonalization of the dynamical matrix yields the eigenfrequencies and the eigenvectors.

3. Results and discussion

Table 1 shows the predicted lattice constants and bulk moduli of $\text{Na}_{16}\text{Rb}_8\text{Ge}_{136}$ and $\text{Na}_{16}\text{Cs}_8\text{Ge}_{136}$. Experimental lattice constants of $\text{Na}_{16}\text{Rb}_8\text{Ge}_{136}$ and $\text{Na}_{16}\text{Cs}_8\text{Ge}_{136}$ are also shown [8, 18]. The predicted lattice constants for the filled clathrates are slightly larger than the LDA calculated lattice constant of 15.13 Å for Ge_{136} [7]². This implies that the completely filled clathrate structures expand due to the inclusion of the guest atoms. Recently, guest-free Ge_{136} has been synthesized with a reported lattice constant of 15.21 Å [19]. The bulk moduli of the filled materials are, however, lower than the predicted bulk modulus of Ge_{136} (61.9 GPa) [7] (see footnote 2). Therefore, the filled Ge clathrates are predicted to be softer than pristine Ge_{136} .

Table 2 shows the calculated and experimental nearest neighbour distances in the two filled clathrates [8, 18]. The small discrepancy between the calculated and experimental Rb–Ge and Na–Ge distances in $\text{Na}_{16}\text{Rb}_8\text{Ge}_{136}$ is consistent with the underestimation of our theoretical lattice constant (15.35 Å) compared to the experimental one (15.48 Å).

Results of the electronic band structure calculations reveal a rigid band character for both $\text{Na}_{16}\text{Rb}_8\text{Ge}_{136}$ and $\text{Na}_{16}\text{Cs}_8\text{Ge}_{136}$. Their band structures are similar to those of the guest-free Ge_{136} [7] (see footnote 2). Unlike Ge_{136} , however, the filled clathrates have their Fermi level (E_f) inside the conduction band and are thus predicted to have metallic character. This

² Our calculations of the structural, electronic and vibrational properties of guest-free Ge_{136} produced similar results to those reported in [7].

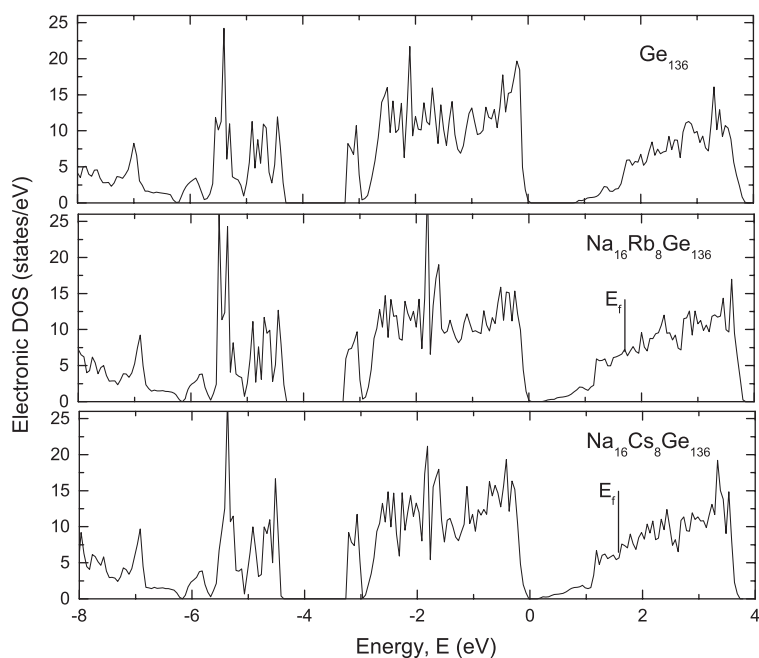


Figure 1. Electronic density of states of Ge_{136} , $\text{Na}_{16}\text{Rb}_8\text{Ge}_{136}$ and $\text{Na}_{16}\text{Cs}_8\text{Ge}_{136}$ in the valence band and the lower portion of the conduction band. The top of the valence band is taken as the zero of energy. The Fermi levels of the filled clathrates are shown by a vertical line.

metallic behaviour agrees qualitatively with the resistivity measurements of $\text{Na}_{16}\text{Rb}_8\text{Ge}_{136}$ and $\text{Na}_{16}\text{Cs}_8\text{Ge}_{136}$ [8, 9].

Figure 1 shows the calculated electronic density of states (DOS) of Ge_{136} , $\text{Na}_{16}\text{Rb}_8\text{Ge}_{136}$ and $\text{Na}_{16}\text{Cs}_8\text{Ge}_{136}$. We find that Ge_{136} is semiconducting with a band gap of about 0.75 eV, in agreement with previous calculations [7]. In the filled clathrates, the Fermi level lies inside the conduction band, as shown by a vertical line in figure 1. The guest atoms in $\text{Na}_{16}\text{Rb}_8\text{Ge}_{136}$ and $\text{Na}_{16}\text{Cs}_8\text{Ge}_{136}$ act as electron donors. Since all framework Ge atoms are covalently bonded, the donated electrons occupy the conduction levels, giving these materials a metallic character.

To emphasize the role of the different guest atoms, we have calculated the s- and p-orbital projected densities of states of Na, Rb and Cs in $\text{Na}_{16}\text{Rb}_8\text{Ge}_{136}$ and $\text{Na}_{16}\text{Cs}_8\text{Ge}_{136}$. Figures 2 and 3 show the projected state densities for Na and Rb in $\text{Na}_{16}\text{Rb}_8\text{Ge}_{136}$ and Na and Cs in $\text{Na}_{16}\text{Cs}_8\text{Ge}_{136}$, respectively. Both figures show the s-orbital character of the states at the bottom of the conduction band, near the Fermi level of each filled clathrate. These s-states come from the delocalized s-electrons of the different guest atoms.

The predicted phonon dispersion curves and vibrational densities of states (VDos) of $\text{Na}_{16}\text{Rb}_8\text{Ge}_{136}$ and $\text{Na}_{16}\text{Cs}_8\text{Ge}_{136}$ are shown in figure 4. In guest-free Ge_{136} , the acoustic modes extend up to about 60 cm^{-1} and the optic modes are in the range $60\text{--}285\text{ cm}^{-1}$ [7] (see footnote 2). The notable feature in the dispersion curves of each of the filled clathrates is the compression of the bandwidth of the heat carrying acoustic phonons from about 60 cm^{-1} in Ge_{136} [7] (see footnote 2) to below 40 cm^{-1} in $\text{Na}_{16}\text{Rb}_8\text{Ge}_{136}$ and $\text{Na}_{16}\text{Cs}_8\text{Ge}_{136}$. This is due to the very flat localized modes from the Rb and Cs guests. Due to an avoided crossing effect, the acoustic branches of the host framework are bent below the localized rattler modes. This could lead to resonant scattering of the highly dispersive host acoustic phonons, potentially reducing the lattice thermal conductivity. In both filled clathrates, the optic bands are approximately

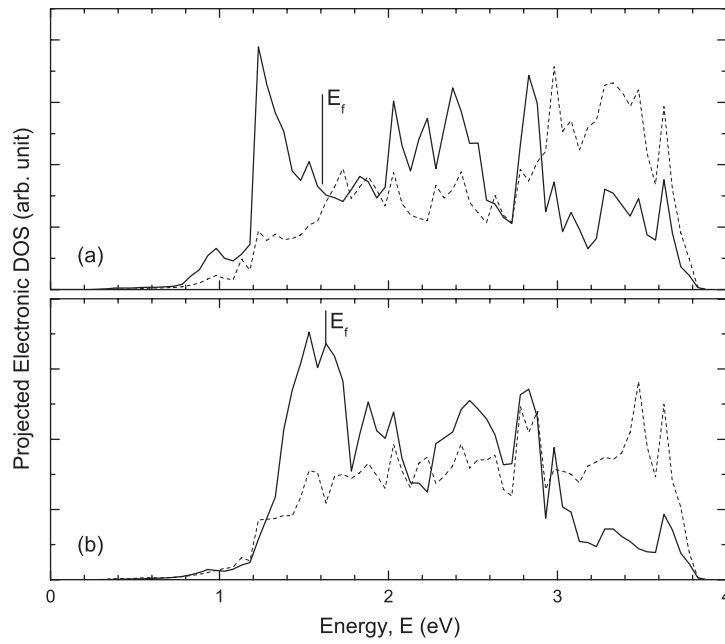


Figure 2. s- (solid curve) and p-orbital (dashed curve) projected density of states for (a) Na and (b) Rb in the lower portion of the conduction band near the Fermi level of the $\text{Na}_{16}\text{Rb}_8\text{Ge}_{136}$ clathrate.

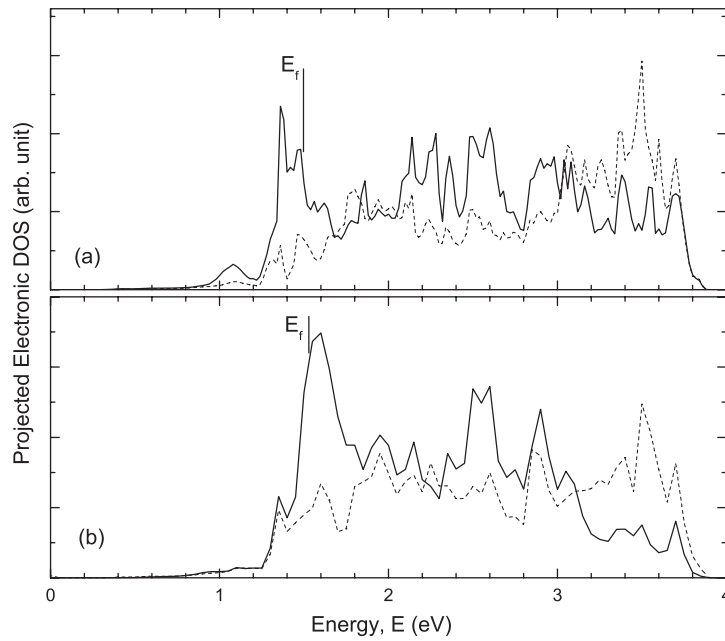


Figure 3. s- (solid curve) and p-orbital (dashed curve) projected density of states for (a) Na and (b) Cs in the lower portion of the conduction band near the Fermi level of the $\text{Na}_{16}\text{Cs}_8\text{Ge}_{136}$ clathrate.

separated into three regions. For example in $\text{Na}_{16}\text{Cs}_8\text{Ge}_{136}$, there is a low frequency, high density of states region from about 40 cm^{-1} to about 80 cm^{-1} , a medium frequency region extending from about 100 cm^{-1} to about 230 cm^{-1} and a narrow, high frequency region from about 230 cm^{-1} to about 250 cm^{-1} .

The phonon dispersion curves in figure 4 show that the high frequency modes in $\text{Na}_{16}\text{Rb}_8\text{Ge}_{136}$ and $\text{Na}_{16}\text{Cs}_8\text{Ge}_{136}$ are down-shifted compared to those in Ge_{136} [7]. In Ge_{136} , the highest frequency extends up to about 285 cm^{-1} [7], whereas in the filled clathrates they are down-shifted to almost 250 cm^{-1} . These high frequency optical branches are due to the bond-stretching modes. In the rigid band picture, the donated electrons from the various guest atoms in $\text{Na}_{16}\text{Rb}_8\text{Ge}_{136}$ and $\text{Na}_{16}\text{Cs}_8\text{Ge}_{136}$ primarily occupy the Ge framework antibonding states. These electrons reduce the Ge–Ge bond order and, therefore, diminish the stretching force of the Ge–Ge bonds [20]. As a result, those bond-stretching modes shift towards lower frequencies, as is seen from our calculations.

One significant difference between the present GGA-based study and an earlier LDA-based study [12] on $\text{Na}_{16}\text{Cs}_8\text{Ge}_{136}$ is the predicted vibrational frequencies of the Na and Cs guests. Based on our GGA calculations, we predict that the Na and Cs modes in $\text{Na}_{16}\text{Cs}_8\text{Ge}_{136}$ are in the ranges $108\text{--}114$ and $40\text{--}42\text{ cm}^{-1}$, respectively. These are in good agreement with the estimated experimental values of 117 cm^{-1} for Na and 41.8 cm^{-1} for Cs in $\text{Na}_{16}\text{Cs}_8\text{Ge}_{136}$ [9]. The previous local density approximation (LDA) calculations of [12] predicted much lower frequencies for Na ($89\text{--}94\text{ cm}^{-1}$) and Cs ($21\text{--}23\text{ cm}^{-1}$) in $\text{Na}_{16}\text{Cs}_8\text{Ge}_{136}$.

The vibrations of the loosely bound guest atoms inside the oversized clathrate cages may be approximately treated as independent Einstein oscillators. At temperatures where $\hbar\omega < 2k_B T$, we can estimate the isotropic atomic displacement parameters of the different guest atoms using the classical expression $U_{\text{iso}} \approx k_B T / K$, where K is the effective force constant of the oscillator and k_B is the Boltzmann constant. The calculated values of U_{iso} can then be used to characterize the localized disorder created by the different guest atoms.

We have estimated the values of K from our calculated frequencies, using the simple relation $\omega = \sqrt{K/M}$. The calculated force constants for Na and Rb in $\text{Na}_{16}\text{Rb}_8\text{Ge}_{136}$ are 1.1 and 0.55 eV \AA^{-2} , respectively. Similarly, in $\text{Na}_{16}\text{Cs}_8\text{Ge}_{136}$ the estimated values for Na and Cs are 0.98 and 0.78 eV \AA^{-2} , respectively. Using these K values, we show in figures 5 and 6 our estimated temperature dependent U_{iso} (discrete symbols) of the different guest atoms in $\text{Na}_{16}\text{Rb}_8\text{Ge}_{136}$ and $\text{Na}_{16}\text{Cs}_8\text{Ge}_{136}$. The experimental U_{iso} of the guests shown in figures 5 and 6 were obtained from [9]. The solid curves in both figures correspond to the U_{iso} calculated in the quantized harmonic oscillator model³. It is evident from figures 5 and 6 that the U_{iso} of the Rb guests in $\text{Na}_{16}\text{Rb}_8\text{Ge}_{136}$ are larger than those of Cs in $\text{Na}_{16}\text{Cs}_8\text{Ge}_{136}$. This is due to the larger K values for Cs than for Rb. The predicted vibrational frequency of Rb in $\text{Na}_{16}\text{Rb}_8\text{Ge}_{136}$ ($\sim 42\text{ cm}^{-1}$) is very close to that of Cs in $\text{Na}_{16}\text{Cs}_8\text{Ge}_{136}$ ($\sim 40\text{ cm}^{-1}$). However, Cs is heavier than Rb, resulting in a larger K and therefore smaller U_{iso} . It is conceivable that the Cs atom, because of its larger size, interacts more strongly with its neighbours, causing it to be more strongly bound than Rb.

Except for Na in $\text{Na}_{16}\text{Rb}_8\text{Ge}_{136}$, the estimated U_{iso} for the guests in both clathrates (figures 5 and 6) are not in very good quantitative agreement with reported experimental data [9]. The disagreement between experiment and our predicted results could be due to anharmonic effects and static disorder. Static disorder would have the effect of shifting the U_{iso} values of the different guests upward. At least in the case of the U_{iso} for Na and Cs in $\text{Na}_{16}\text{Cs}_8\text{Ge}_{136}$, static disorder is believed to be the more likely cause, because the slopes of the temperature dependent lines in figure 6 are similar to those of the experiment. Our

³ In the quantized harmonic oscillator model, $U_{\text{iso}} = \langle u^2 \rangle = \frac{\hbar}{8\pi^2 m \nu} \coth\left(\frac{\hbar\nu}{2k_B T}\right)$ [21].

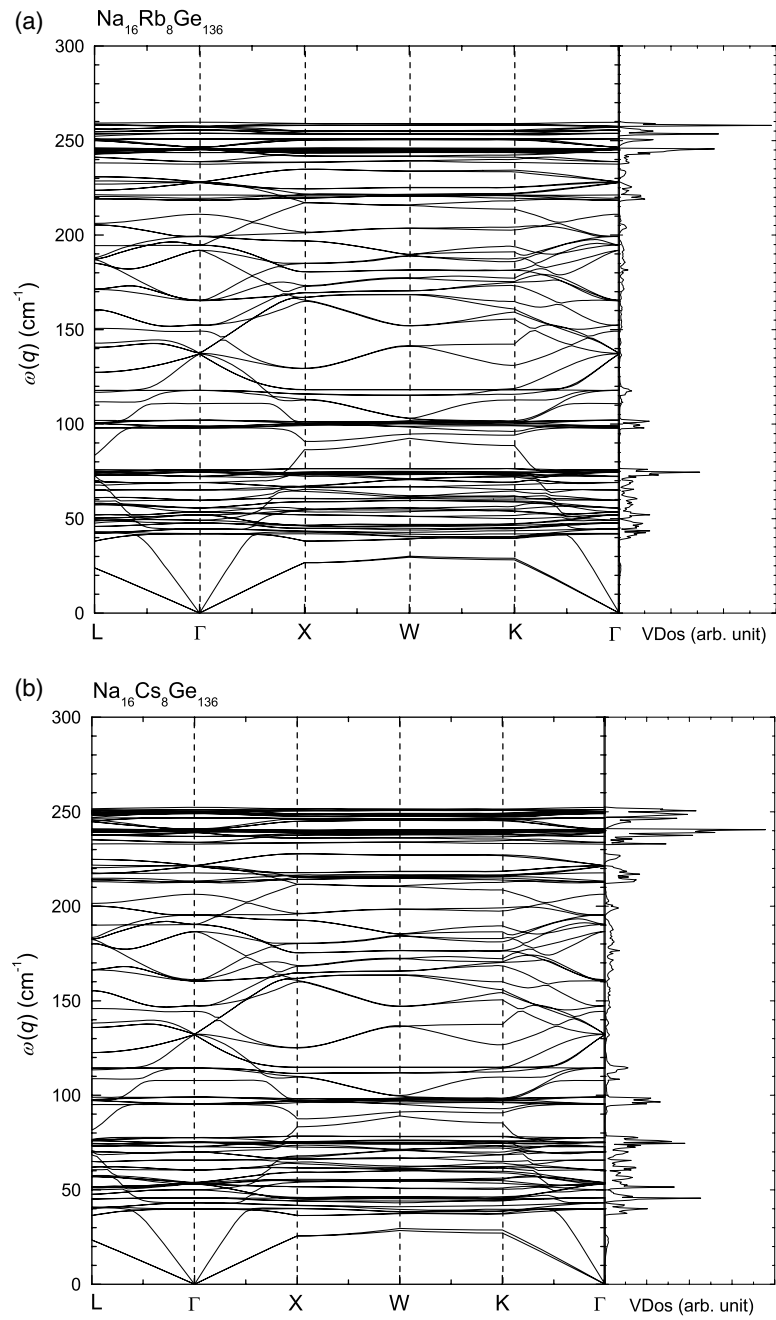


Figure 4. Phonon dispersion relations and vibrational density of states (VDos) of (a) $\text{Na}_{16}\text{Rb}_8\text{Ge}_{136}$ and (b) $\text{Na}_{16}\text{Cs}_8\text{Ge}_{136}$.

predicted values of U_{iso} also give the correct trend, where the smaller and lighter Rb atoms in $\text{Na}_{16}\text{Rb}_8\text{Ge}_{136}$ are predicted to have larger U_{iso} compared to the heavier Cs atoms in $\text{Na}_{16}\text{Cs}_8\text{Ge}_{136}$.

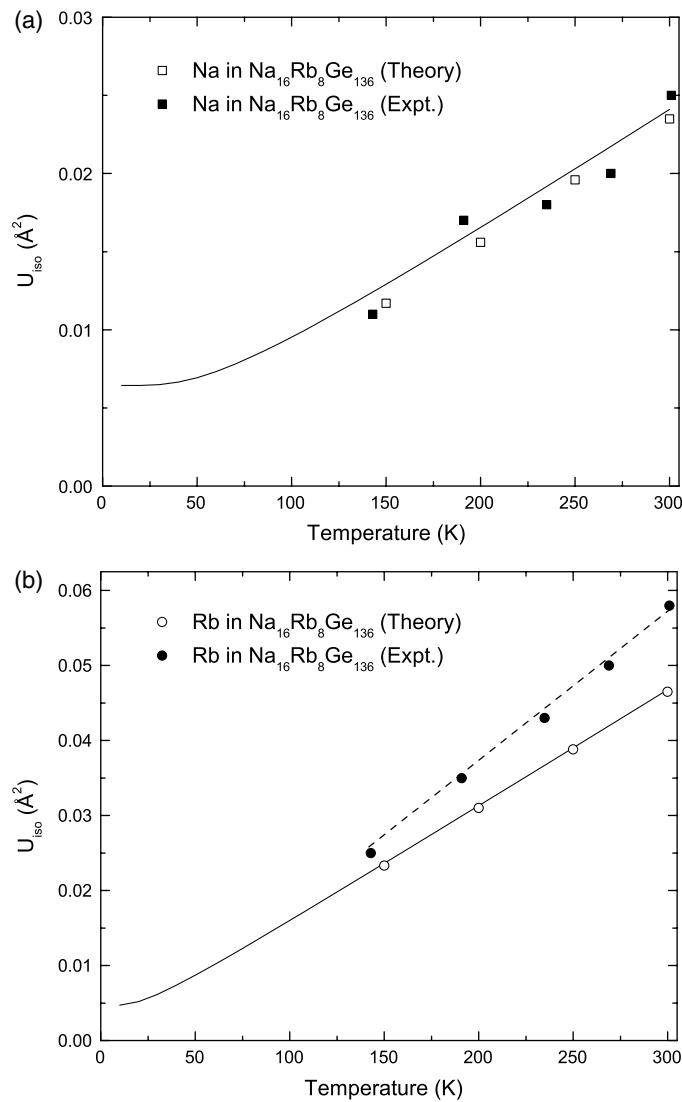


Figure 5. Estimated theoretical (open symbols) and experimental [9] values (solid symbols) of the isotropic atomic displacement parameters (U_{iso}) of (a) Na and (b) Rb in $\text{Na}_{16}\text{Rb}_8\text{Ge}_{136}$ at different temperatures. The solid curves are plots of U_{iso} based on the quantized harmonic oscillator model [21].

The predicted U_{iso} of the guest atoms in the Ge clathrates are larger than those in the Si clathrates [22], in agreement with experiment [9]. This is expected because of the slightly smaller cage sizes in the Si clathrates. Hence, the guest atoms in the Si clathrate cages are more strongly bound, which leads to smaller U_{iso} than those in the Ge-based materials.

4. Conclusions

We have used the GGA to study the electronic and vibrational properties of the Ge-based type-II clathrates, $\text{Na}_{16}\text{Rb}_8\text{Ge}_{136}$ and $\text{Na}_{16}\text{Cs}_8\text{Ge}_{136}$. The electronic properties show a charge transfer

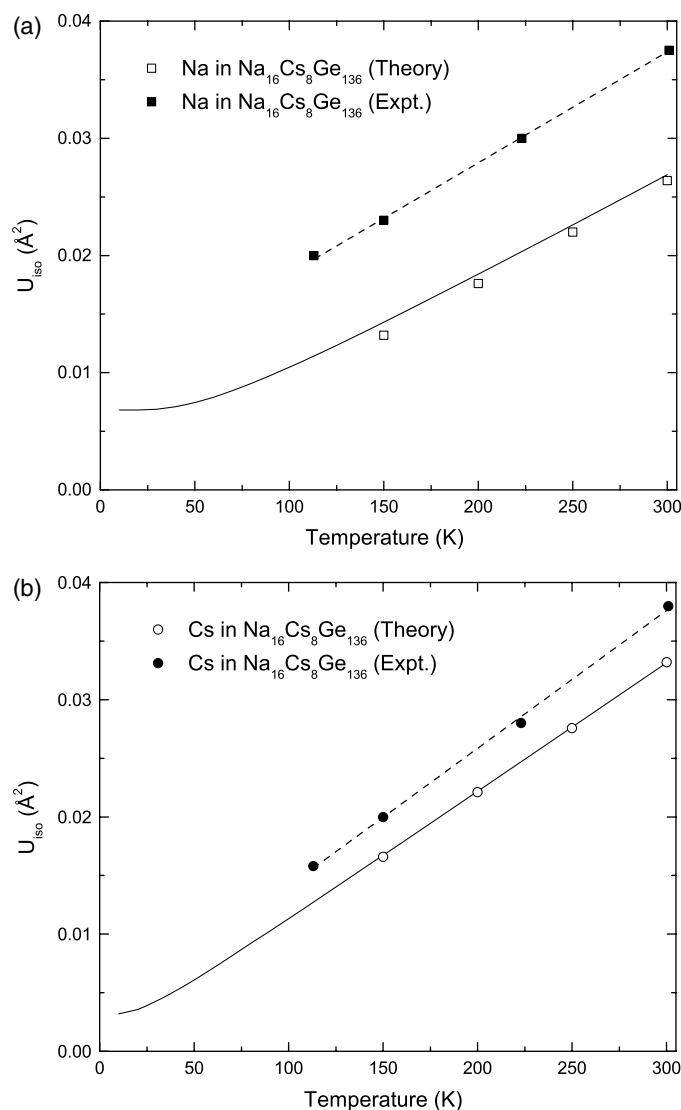


Figure 6. Estimated theoretical (open symbols) and experimental [9] values (solid symbols) of the isotropic atomic displacement parameters (U_{iso}) of (a) Na and (b) Cs in $\text{Na}_{16}\text{Cs}_8\text{Ge}_{136}$ at different temperatures. The solid curves are plots of U_{iso} based on the quantized harmonic oscillator model [21].

from the guest atoms to the framework conduction band, effectively making these materials metallic. The projected electronic densities of states of the different guest atoms show the s-orbital character of the states near the Fermi level at the bottom of the conduction band of each material. This is due to the delocalized s-electrons from the guest atoms. The GGA predicted vibrational frequencies are in good agreement with estimated experimental values. Previous work on $\text{Na}_{16}\text{Cs}_8\text{Ge}_{136}$, which was based on the LDA, predicted very low Na and Cs frequencies [12]. Such low frequencies lead to very low force constants (K) and very high U_{iso} . The present GGA results are in better agreement with experiment.

Acknowledgments

We thank M Sanati (Texas Tech University) for helpful discussions on the use of VASP for our calculations. We acknowledge generous CPU time made available to us by the High Performance Computer Center at Texas Tech University.

References

- [1] Slack G A 1979 *Solid State Physics* vol 34, ed H Ehrenreich, F Seitz and D Turnbull (New York: Academic)
- Slack G A 1995 *CRC Handbook of Thermoelectrics* ed D M Rowe (Boca Raton, FL: CRC Press) p 407
- [2] Nolas G S, Slack G A and Schujman S B 2001 *Semiconductors and Semimetals* vol 69, ed T M Tritt (San Diego, CA: Academic) p 255 and references therein
- [3] Kasper J S, Hagemuller P, Pouchard M and Cros C 1965 *Science* **150** 1713
- [4] Mélinon P, Kéghélian P, Blasé X, Brusca J Le, Perez A, Reny E, Cros C and Pouchard M 1998 *Phys. Rev. B* **58** 12590
- [5] Mélinon P, Kéghélian P, Perez A, Champagnon B, Guyot Y, Saviot L, Reny E, Cros C, Pouchard M and Dianoux A J 1999 *Phys. Rev. B* **59** 10099
- [6] Dong J, Sankey O F and Kern G 1999 *Phys. Rev. B* **60** 950
- [7] Dong J and Sankey O F 1999 *J. Phys.: Condens. Matter* **11** 6129
- [8] Bobev S and Sevov S C 2000 *J. Solid State Chem.* **153** 92
- [9] Nolas G S, Vanderveer D G, Wilkinson A P and Cohn J L 2002 *J. Appl. Phys.* **91** 8970
- [10] Gryko J, McMillan P F, Marzke R F, Dodokin A P, Demkov A A and Sankey O F 1998 *Phys. Rev. B* **57** 4172
- [11] Gryko J, Marzke R F, Lamberton G A Jr, Tritt T M, Beekman M and Nolas G S 2005 *Phys. Rev. B* **71** 115208
- [12] Myles C W, Dong J and Sankey O F 2003 *Phys. Status Solidi b* **239** 26
- [13] Vanderbilt D 1990 *Phys. Rev. B* **41** 7892
- Laasonen K, Car R, Lee C and Vanderbilt D 1991 *Phys. Rev. B* **43** 6796
- Laasonen K, Pasquarello A, Car R, Lee C and Vanderbilt D 1993 *Phys. Rev. B* **47** 10142
- [14] Kresse G and Furthmüller J 1996 *Comput. Mater. Sci.* **6** 15
- Kresse G and Hafner J 1993 *Phys. Rev. B* **47** 558
- Kresse G and Furthmüller J 1996 *Phys. Rev. B* **54** 11169
- [15] Perdew J P 1991 *Electronic Structure of Solids '91* ed P Ziesche and H Eschrig (Berlin: Akademie Verlag)
- Perdew J P, Chevary J A, Vosko S H, Jackson K A, Pederson M R, Singh D J and Fiolhais C 1992 *Phys. Rev. B* **46** 6671
- [16] Monkhorst H J and Pack J D 1976 *Phys. Rev. B* **13** 5188
- [17] Birch F 1952 *J. Geophys. Res.* **57** 227
- [18] Bobev S and Sevov S C 1999 *J. Am. Chem. Soc.* **121** 3795
- [19] Guloy A M, Ramlau R, Tang Z, Schnelle W, Baitinger M and Grin Y 2006 *Nature* **443** 320
- [20] Nolas G S, Kendziora C A, Gryko J, Dong J, Myles C W, Poddar A and Sankey O F 2002 *J. Appl. Phys.* **92** 7225
- [21] Dunitz J D, Schomaker V and Trueblood K N 1988 *J. Phys. Chem.* **92** 856
- [22] Biswas K and Myles C W 2007 *Phys. Rev. B* **75** 245205